Development 125, 5091-5104 (1998)
Printed in Great Britain © The Company of Biologists Limited 1998
DEV1351

Visceral endoderm-restricted translation of *Otx1* mediates recovery of *Otx2* requirements for specification of anterior neural plate and normal gastrulation

Dario Acampora[1], Virginia Avantaggiato[1], Francesca Tuorto[1], Paola Briata[2], Giorgio Corte[2] and Antonio Simeone[1,*]

[1]International Institute of Genetics and Biophysics, CNR, Via G. Marconi 12, 80125 Naples, Italy
[2]National Institute for Cancer Research-CBA, Dipartimento di Oncologia Clinica e Sperimentale, Università di Genova, Largo Benzi, 16132 Genova, Italy
*Author for correspondence (e-mail: simeone@iigbna.iigb.na.cnr.it)

Accepted 11 October; published on WWW 12 November 1998

SUMMARY

***Otx1* and *Otx2*, two murine homologs of the *Drosophila orthodenticle (otd)* gene, contribute to brain morphogenesis. In particular *Otx1* null mice are viable and show spontaneous epileptic seizures and abnormalities affecting the dorsal telencephalic cortex. *Otx2* null mice die early in development and fail in specification of the rostral neuroectoderm and proper gastrulation. In order to determine whether $Otx1^{-/-}$ and $Otx2^{-/-}$ highly divergent phenotypes reflect differences in temporal expression or biochemical activity of OTX1 and OTX2 proteins, the *Otx2*-coding sequence was replaced by a human *Otx1* full-coding cDNA. Homozygous mutant embryos recovered anterior neural plate and proper gastrulation but failed to maintain forebrain-midbrain identities, displaying a headless phenotype from 9 days post coitum (d.p.c.) onwards. Unexpectedly, in spite of the RNA distribution in both visceral endoderm (VE) and epiblast, the hOTX1 protein was synthesized only in the VE. This VE-restricted translation was sufficient to recover *Otx2* requirements for specification of the anterior neural plate and proper organization of the primitive streak, thus providing evidence that the difference between *Otx1* and *Otx2* null mice phenotypes originates from their divergent expression patterns.**

Moreover, our data lead us to hypothesize that the differential post-transcriptional control existing between VE and epiblast cells may potentially contribute to fundamental regulatory mechanisms required for head specification.

Key words: Visceral endoderm, Epiblast, Gastrulation, Head specification, *Otx1*, *Otx2*, Translation

INTRODUCTION

A large body of evidence indicates that fate and patterning of tissues depend on the activity of organizer cells emanating signals to a responding tissue which undergoes morphogenetic changes resulting in a specific differentiated fate (Spemann and Mangold, 1924; Waddington, 1932; Gurdon, 1987). When induced by an organizer, responding ectoderm undergoes morphogenetic changes and gives rise to an early neural plate (Spemann and Mangold, 1924; Waddington, 1932). The early neural plate is then transformed into a neural tube composed of large anteroposterior domains with distinct fates corresponding to the prosencephalon, mesencephalon and rhomboencephalon. Early specification and patterning of the CNS primordium is controlled by distinct mechanisms involving vertical signals from axial mesendoderm underlying the neural plate and planar signals acting through the neuroectodermal plane (Doniach, 1993; Ruiz i Altaba, 1993, 1994, 1998; Houart et al., 1998; Rubenstein et al., 1998). However, new and ever-increasing data indicate that the anterior visceral endoderm (AVE) in mouse and the leading edge of the involuting endoderm in *Xenopus* both play a crucial role in early head organizer activity (Bouwmeester et al., 1996; Thomas and Beddington, 1996; Varlet et al., 1997).

In vertebrates, most of the genes likely to execute morphogenetic programs underlying brain morphogenesis are the homologs of *Drosophila* genes coding for signal molecules or transcription factors (Lemaire and Kodjabachian, 1996; Rubenstein et al., 1998; Tam and Behringer, 1997). Among these, the *orthodenticle* group is defined by the *Drosophila orthodenticle (otd)* and the vertebrate *Otx1*, *Otx2* and *Crx* genes, which contain a *bicoid*-like homeodomain (Finkelstein and Boncinelli, 1994; Chen et al., 1997; Freud et al., 1997). Murine *Otx1* and *Otx2* gene products share extensive sequence similarities even though in *Otx1*, downstream of the homeodomain, these regions of homology to OTX2 are separated by stretches of additional aminoacids including repetitions of alanine and histidine residues (Simeone et al., 1993). In mouse, *Otx1* expression is first detected at the 1- to 3-somite stage throughout the forebrain and midbrain

neuroepithelium. *Otx2* is already transcribed before the onset of gastrulation in the epiblast and in the visceral endoderm (VE) and, at the end of gastrulation, in the axial mesendoderm and rostral rostral neural plate (Simeone et al., 1992, 1993). During brain regionalization, *Otx1* and *Otx2* show largely overlapping expression domains with a posterior border coincident with the mesencephalic side of the isthmic constriction (Simeone et al., 1992; Millet et al., 1996; Acampora et al., 1997). Furthermore, *Otx1* is transcribed in neurons of deep layers of the adult cerebral cortex (Frantz et al., 1994). *Otx1* null mice show spontaneous epileptic seizures and multiple abnormalities affecting proper brain and sense organs development as well as pituitary functions (Acampora et al., 1996, 1998). *Otx2* null mice die early in embryogenesis, show heavy gastrulation abnormalities affecting VE, primitive streak and axial mesendoderm, and fail to specify rostral neuroectoderm fated to give forebrain, midbrain and rostral hindbrain (Acampora et al., 1995; Matsuo et al., 1995; Ang et al., 1996).

Hence, on the basis of mutant phenotypes and expression patterns, *Otx2* is required for proper gastrulation and specification of an early neural plate when *Otx1* expression is still off, and, at a later stage, *Otx1* is required primarily in the dorsal telencephalon where *Otx2* is not transcribed. Therefore, these findings support two hypotheses: (i) *Otx1* and *Otx2* functional properties might largely overlap and differences in their temporal and spatial transcriptional control might account for the highly divergent phenotypes observed in mice lacking *Otx1* or *Otx2*, or (ii) *Otx1* and *Otx2* gene products might display unique functional properties, specified by their limited aminoacid divergence, that are required in restricted tissue domains at specific developmental stages.

In order to distinguish between these two possibilities, we generated by homologous recombination a mouse model in which the *Otx2*-coding sequence was replaced by a human *Otx1 (hOtx1)* full-coding cDNA. $hOtx1^2/hOtx1^2$ embryos rescued a normal body axis and an early neural plate but failed to maintain the anterior patterning. Moreover, while the *hOtx1* transcripts were detected in both VE and epiblast, in contrast, the hOTX1 protein was restricted to the VE. Interestingly, the VE-restricted hOTX1 protein was able to rescue OTX2 requirements for specification and initial patterning of the early neural plate as well as for proper organization of the primitive streak, providing in vivo evidence that OTX1 properties might share extensive functional similarities with those encoded by the OTX2 protein in the VE and that a differential post-transcriptional control, unmasked by the *hOtx1* chimaeric transcript, exists between VE and epiblast cells. The latter may potentially represent a crucial regulatory aspect in the morphogenetic process required for head specification.

MATERIALS AND METHODS

Targeting vector, ES cell transfection and selection of targeted clones

The gene replacement vector was generated from the same plasmid (pGN31) used to produce $Otx2^{-/-}$ mice (Acampora et al., 1995). A *Sma*I-*Hin*dIII fragment of the *hOtx1* cDNA was cloned in place of the *lacZ* gene by digestion of the unique *Sac*II-*Nde*I sites flanking the bacterial gene in the former targeting vector. As in the *Otx2* knock-out vector, a SV40 polyadenylation signal was present downstream of the cDNA to ensure transcription termination. 15 μg of targeting vector were linearized by *Kpn*I digestion and electroporated into 2×10^7 HM-1 ES cells. Homologous recombinant clones were identified using the same primers as previously described (Acampora et al., 1995) (filled arrows in Fig. 1A) and confirmed by hybridizing *Hin*dIII-digested genomic DNA with probes (A) and (E) (Fig. 1A).

Mouse production and genotyping

Two independent positive clones were injected into C57BL/6 blastocysts and the resulting chimaeric males back-crossed to B6/D2 F_1 females. Genotyping was performed by PCR using two primers specific for the wild-type allele and located in the *Otx2*-deleted sequence (sense primer, GTGACTGAGAAACTGCTCCC; antisense primer, GTGTCTACATCTGCCCTACC) (filled arrowheads in Fig. 1A) and two primers specific for the *hOtx1* cDNA (sense primer, GATGTGCAAACCCACCCTGCCC; antisense primer, TGCGCGG-GAGGAACTCTTAGT) (open arrowheads in Fig. 1A).

RNase protection assay and probes

RNase protection was performed as previously described (Simeone et al., 1993). The *hOtx1* probe was a 220 bp long *Xba*I-*Pst*I fragment deriving from the cDNA.

The mouse *Otx1* probe was a genomic *Pvu*II-*Bgl*II 166 bp long fragment containing part of the second exon and of the second intron.

The probe for mouse *Otx2* was a genomic *Hae*III 142 bp long fragment containing part of the first exon and of the first intron.

Western blot analysis

Nuclear extracts were prepared from 10.5 d.p.c. heads. 50 μg of these extracts and 10 μg of nuclear extracts of HeLa cells transfected with plasmids overexpressing human *Otx1* and *Otx2* cDNAs under a CMV enhancer-promoter (Simeone et al., 1993) were electrophoresed and transferred to nitrocellulose in a standard western blot assay and probed with αOTX2, αOTX1 and αOTX1p antisera (1:5000, 1:3000, 1:1000, respectively). 50 μg of ES cells extract were probed with αOTX2 antibody diluted 1:5000.

Immunohistochemistry and αOTX1 preabsorption

Gastrulating embryos were fixed in 4% paraformaldehyde and embedded in wax following the same procedure as for in situ hybridization with ^{35}S RNA probes (Wilkinson, 1992).

Adjacent sections were then processed either for RNA hybridization or for immunohistochemistry. Two polyclonal antisera directed against OTX2 (Mallamaci et al., 1996) and OTX1 proteins were employed. The latter was generated following the same procedure previously shown for the αOTX2 (Mallamaci et al., 1996).

For immunohistochemistry, sections were deparaffinized in Bio-Clear, rehydrated and incubated at room temperature with the polyclonal antisera (αOTX2 or αOTX1 or αOTX1p) (1:1000 or 1:1500 or 1:500 in PBS, 10% fetal calf serum) overnight. The rest of the manipulations were performed according to the streptavidin-biotin-horseradish peroxidase (HRP) complex technique using a kit system (Dako, Glostrup, Denmark). To eliminate as much cross-reactivity with the OTX2 protein as possible, the αOTX1 antiserum was preabsorbed with pure recombinant OTX2 protein coupled to Sepharose 4B.

In situ hybridization and probes

In situ hybridization experiments on sections and whole embryos were performed as previously described (Wilkinson, 1992; Hogan et al., 1994) using ^{35}S-labelled and digoxigenin-labelled RNA probes, respectively.

The *Wnt1*, *Pax2* and *Fgf8* probes are the same as previously described (Acampora et al., 1997). The *En1* probe is a PCR fragment including the region between aa 112 and aa 260 (Logan et al., 1992). The *Gbx2* probe is a PCR fragment including the region between aa

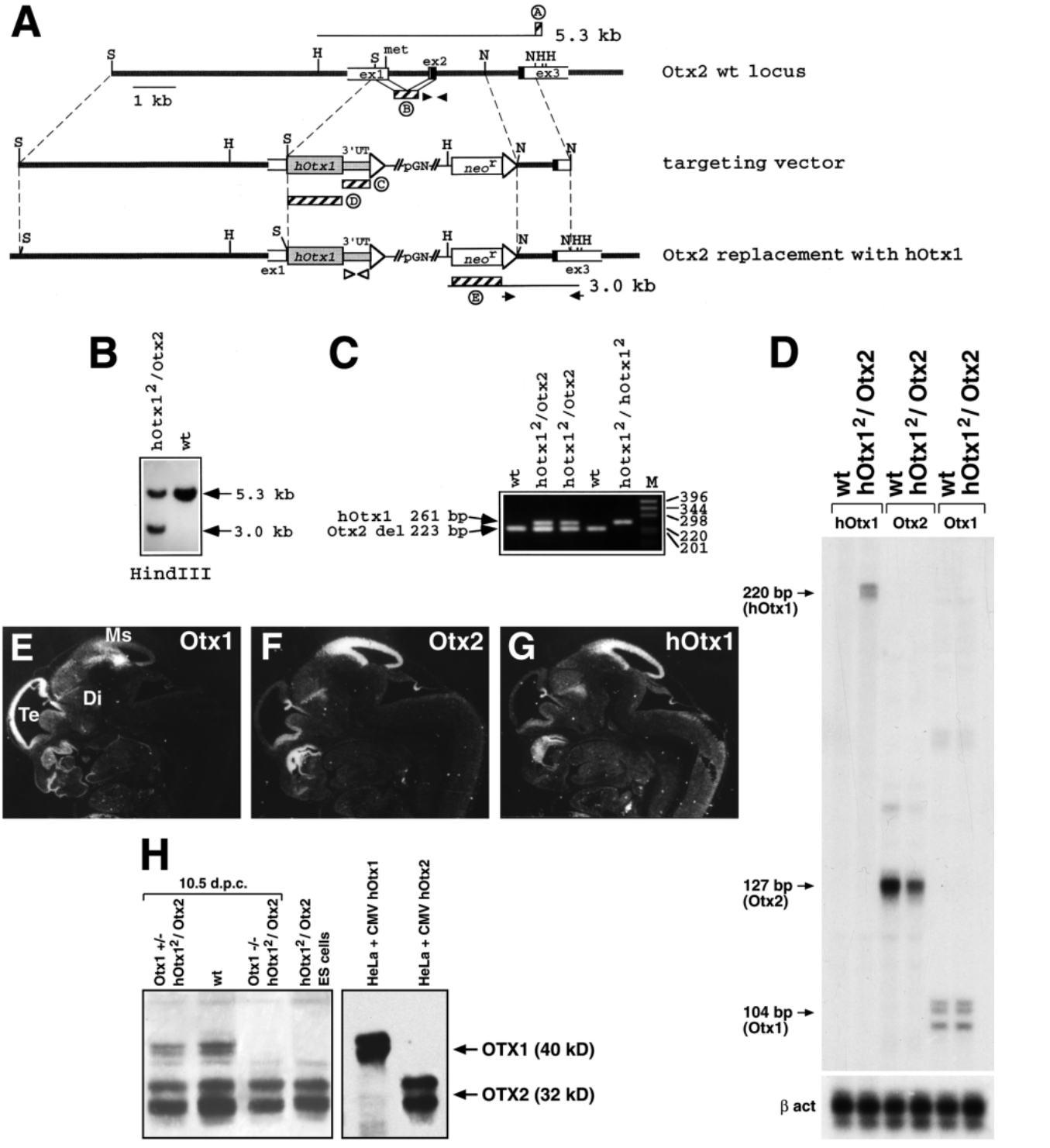

Fig. 1. Targeted replacement of *Otx2* with *hOtx1* cDNA, transcription and translation of *hOtx1* in embryos and ES cells. (A) Targeting vector shown in third line. Fourth line illustrates recombined locus. First and last lines show *Hin*dIII fragments (5. 3 and 3. 0 kb) detected by Southern blot using probes (hatched boxes) external to the targeting vector or within *neomycin* gene. N, H, S stand for *Nsi*I, *Hin*dIII and *Sma*I. (B) Southern blot analysis of one targeted cell line (*hOtx1*^{2}*/Otx2)* and wild-type (wt) HM-1 ES cells showing expected hybridization pattern of *Hin*dIII digested genomic DNA samples with probe A (A). Only the 3. 0 kb fragment is detected with the neo-specific probe (probe E) (data not shown). (C) Genotyping of a litter from mating of two heterozygotes by PCR reaction amplifying fragments specific for the deleted region of *Otx2* (223 bp) and/or *hOtx1* (261 bp), using the primers indicated as filled and open arrowheads in A. (D) RNase protection experiments on wild-type and *hOtx1*^{2}*/Otx2* embryos performed with allele-specific probes (see also Material and Methods). The β-actin RNA represent a quantitative and qualitative control of the RNA. (E-G) *hOtx1* transcripts distribution compared to that of *Otx2* and *Otx1* genes in 12. 5 d.p.c. *hOtx1*^{2}*/Otx2* embryos. *Otx2* and *hOtx1* probes correspond to probes B and C (A), respectively. (H) Western blot analysis of OTX1 and OTX2 proteins in embryonic head and cell extracts. Abbreviations: Te, telencephalon; Di, diencephalon; Ms, mesencephalon.

6 and aa 294 (Chapman et al., 1997). The *Six3* probe is a PCR fragment including the region between aa 97 and aa 352 (Oliver et al., 1995). The *BF1* probe is a PCR fragment including the region between aa 273 and aa 481 plus 198 bp downstream the TGA (Li et al., 1996). The *Noggin* probe is a PCR fragment including the full coding sequence plus 212 bp upstream the AUG (McMahon et al., 1998). The *Lim1* probe is a PCR fragment including the full coding sequence plus 52 bp and 58 bp, respectively, located upstream and downstream the coding sequence (Barnes et al., 1994).

Transcripts from the *Otx2* wild-type allele were revealed by using the probe B (Fig. 1A) which includes 107 bp and 190 bp upstream and downstream the AUG, respectively. Probe C (Fig. 1A) is a 630 bp fragment included in the 3′ UT of the *hOtx1* cDNA that was employed in embryos older than 8-8.5 d.p.c. to prevent cross-hybridization to the endogenous *Otx1* transcripts. Probe D (Fig. 1A) is a 1 kb fragment containing all the coding region of the *hOtx1* cDNA. The probe for the endogenous *Otx1* and *lacZ* genes are the same as previously described (Simeone et al., 1993; Acampora et al., 1995).

RESULTS

Generation of mice replacing *Otx2* with the *hOtx1* cDNA

To assess functional conservation between OTX1 and OTX2 proteins, a human *Otx1* (*hOtx1*) cDNA fused to the SV40 poly(A) of the pGN targeting vector was introduced into a disrupted *Otx2* locus by homologous recombination in embryonic stem (ES) cells (Fig. 1A). The *Otx2* deletion corresponded to a 2.7 kb fragment including ~200 bp of the 5′ UT region immediately upstream of the methionine and the coding region of exons 1 and 2 (Fig. 1A) (Acampora et al., 1995). The targeting vector (Fig. 1A) was constructed with the same DNA fragments previously used for the *Otx2* knock-out (Acampora et al., 1995), but with the *hOtx1*-SV40 poly(A) cassette in place of the *E. coli lacZ* gene. The *hOtx1* cDNA, containing the entire coding region plus 43 and 675 bp of 5′ and 3′ UT sequences, respectively, was fused downstream of the partially deleted *Otx2* 5′ UT sequence. The protein encoded by the *hOtx1* gene differs from its murine counterpart by 9 aminoacid substitutions (four of which are conservative) and the deletion of a single histidine residue into a stretch of 11 in the mouse (Simeone et al., 1993). The gene replacement vector was introduced into HM-1 ES cells and two independent homologous recombinant clones (Fig. 1B and Materials and Methods) were selected and injected into C57BL/6 blastocystes to generate chimaeric mice for germline transmission of the mutated allele. The resulting heterozygotes *(hOtx1^2/Otx2)* were healthy and fertile and their genotypes were determined by allele-specific PCR reactions (Fig. 1C).

Correct expression of *hOtx1* under the *Otx2* transcriptional

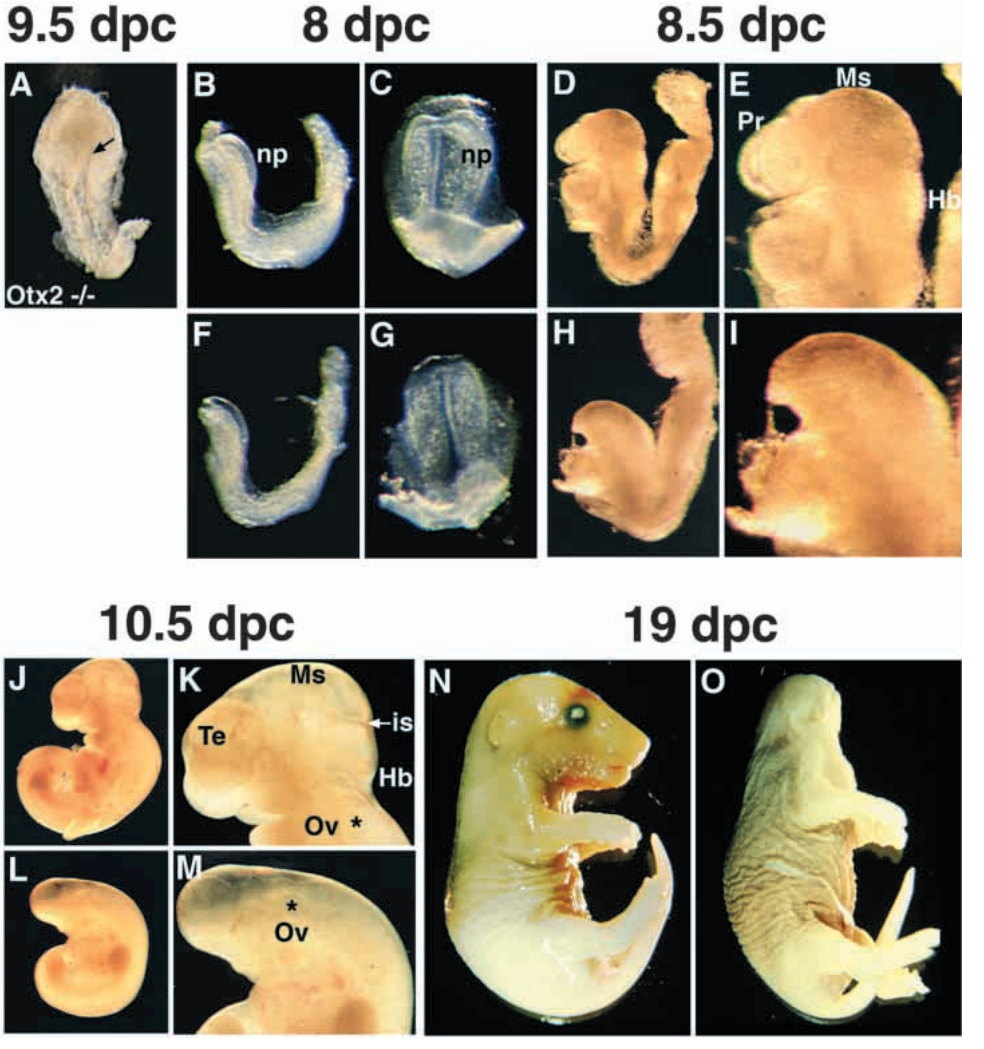

Fig. 2. Morphology of the *hOtx1^2/hOtx1^2* embryos during development. As compared to *Otx2$^{-/-}$* embryos (A) and wild-type embryos (B-E,J,K,N), *hOtx1^2/hOtx1^2* (F-I,L,M,O) embryos show only a slight reduction of the neural plate at 8 d.p.c. (F,G) while, at 8. 5 d.p.c. (H,I), they lack the prosencephalic territory and at 10. 5 d.p.c. (L,M) the forebrain-midbrain areas. Frequently the lack of head structures is accompanied by a heavy reduction of branchial arches (L,M). ~35% of the expected mutant embryos reach the end of gestation showing a normal body axis and loss of anterior head structures (O). Abbreviations as in the previous figure plus: Pr, prosencephalon; Hb, hindbrain; np, neural plate; is, isthmus; Ov, otic vescicle; the arrow in (A) points to the rostral limit of the neural tube and the asterisk in (K,M) is inserted in the otic vescicle.

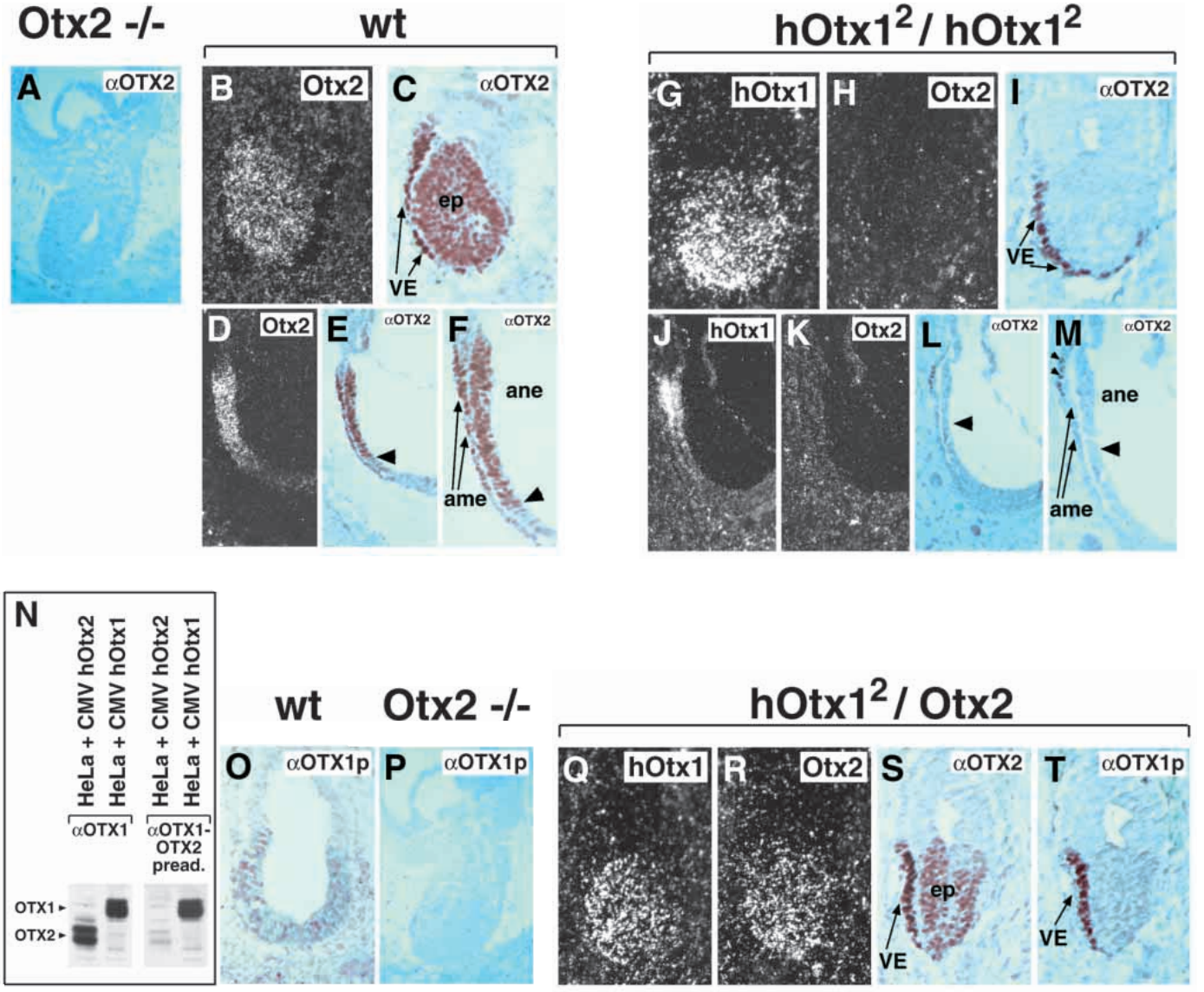

Fig. 3. *hOtx1* and *Otx2* transcript and protein distribution. (A) Specificity of αOTX2 in *Otx2*$^{-/-}$ embryos. (B-F) In wild-type embryos *Otx2* mRNA (B,D) and protein (C,E,F) colocalize in the epiblast and VE at 6. 5 d.p.c. (B,C) and in the neuroectoderm and axial mesendoderm at 7. 75 d.p.c. (E,F). (G-M) Genotype of the *hOtx1*^{2}/*hOtx1*^{2} embryos is determined by hybridization with *hOtx1* and *Otx2* allele-specific probes (G,H,J,K). *hOtx1* transcripts are detected in the VE and epiblast at 6. 5 d.p.c. (G) and in the neuroectoderm and axial mesendoderm at 7. 75 d.p.c. (J) while the hOTX1 protein is restricted to the VE at 6. 5 d.p.c. (I) and to a few cells, possibly residual VE cells, at 7. 75 d.p.c. (L and small arrowheads in M). (N) Western blot of OTX1 and OTX2 proteins with αOTX1 before and after preabsorption to OTX2 protein. (O-P) The αOTX1p reveals a very faint staining in 6. 5 d.p.c. wild-type embryos (O) and no signal in *Otx2*$^{-/-}$ embryos (P). (Q-T) Adjacent sections from *hOtx1*^{2}/*Otx2* 6. 5 d.p.c. embryo show that *hOtx1* (Q) and *Otx2* (R) transcripts colocalize; in contrast, while the αOTX2 (S) reveals high protein level in epiblast and VE, the αOTX1p (T) detects high protein level only in the VE. (F), (M) Magnifications of E, L, respectively. Abbreviations: VE, visceral endoderm; ep, epiblast; ane, anterior neuroectoderm; ame, axial mesendoderm. The arrowheads in E,F,L,M correspond to the posterior border of *Otx2* (E,F) and *hOtx1* (L,M) transcripts.

control was monitored by comparing the level and spatial distribution between *Otx2* and *hOtx1* transcripts in 10.5 and 12.5 d.p.c. *hOtx1*^{2}/*Otx2* embryos (Fig. 1D-G), respectively. RNase protection assay, by using allele-specific probes (see Materials and Methods) and densitometric scanning, indicated a 20-25% reduction of the *hOtx1* transcript level as compared to that of the endogenous *Otx2* (Fig. 1D). In situ hybridization experiments performed on adjacent sections from 12.5 d.p.c. heterozygous embryo indicated that the mRNA distribution of the *hOtx1* allele (probe C in Fig. 1A) colocalized with that of the normal *Otx2* allele (probe B in Fig. 1A) (Fig. 1F,G), while the transcripts of the endogenous *Otx1* appeared unaltered (Fig. 1D,E). Translation of *hOtx1* transcripts was monitored by using an OTX2 polyclonal antibody recognizing in a western blot assay OTX1 and OTX2 proteins with the same efficiency as shown in HeLa cell extracts transfected with expression vectors for *hOtx1* and human *Otx2* (*hOtx2*) (Fig. 1H). Surprisingly, by comparing nuclear extracts from wild-type, *hOtx1*^{2}/*Otx2;*

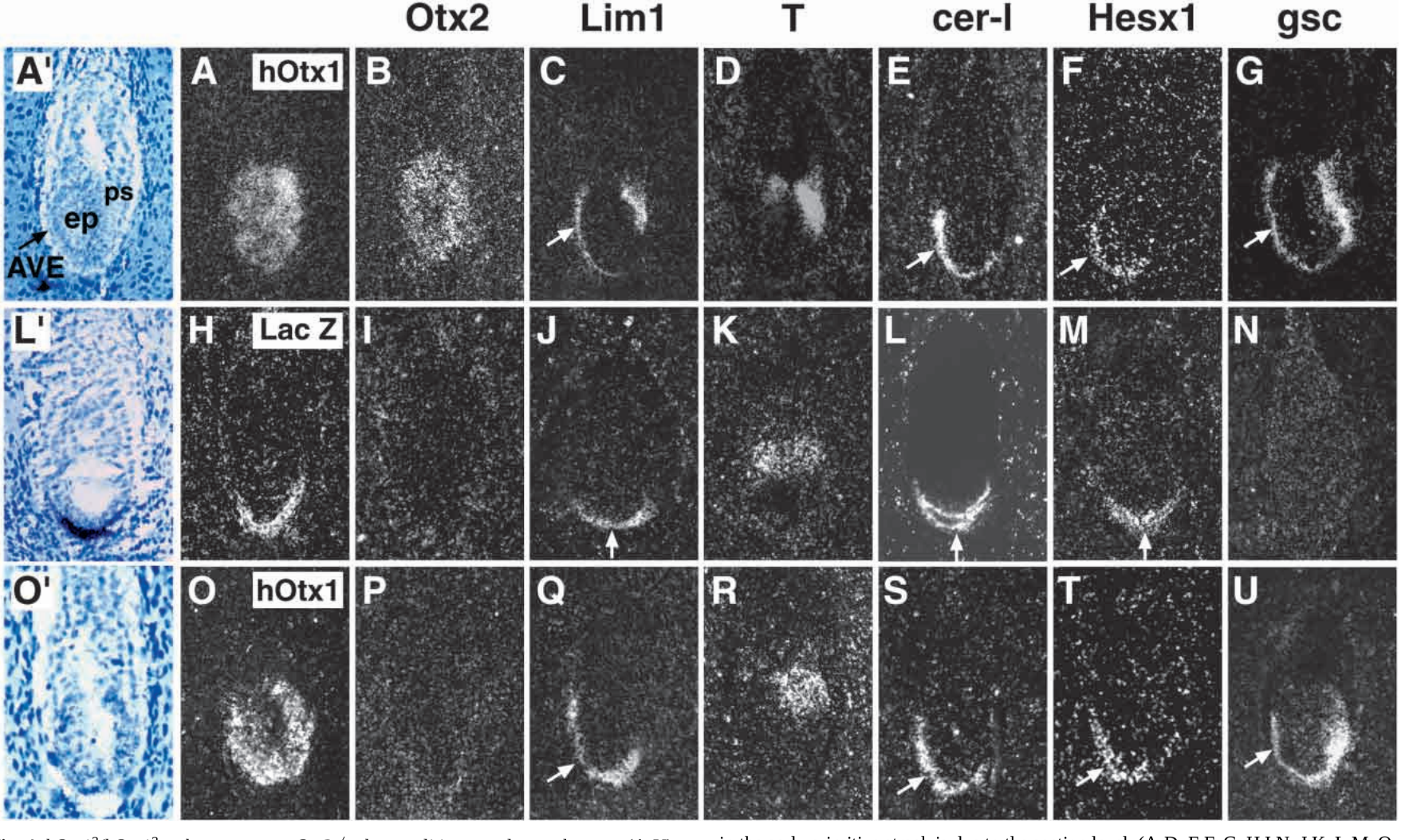

Fig. 4. *hOtx1*^{2}*/hOtx1*^{2} embryos recover *Otx2*$^{-/-}$ abnormalities at early streak stage. (A-U) Sagittal sections of 6. 5 d.p.c. *hOtx1*^{2}*/Otx2* (A-G), *Otx2*$^{-/-}$ (H-N) and *hOtx1*^{2}*/hOtx1*^{2} (O-U) embryos hybridized with *hOtx1* (A,O), *lacZ* (H), *Otx2* (B,I,P), *Lim1* (C,J,Q), *T* (D,K,R), *cer-l* (E,L,S), *Hesx1* (F,M,T) and *gsc* (G,N,U). (Q) The absence of *Lim1* signal in the early primitive streak is due to the section level. (A-D, E,F, G, H,I,N, J,K, L,M, O-Q, R-T and U) Single or group of sections belonging to different embryos. Bright fields of the same sections are labelled with a prime (′). Abbreviations as in the previous figures plus: AVE, anterior visceral endoderm; ps, primitive streak.

Otx1$^{+/-}$ and *hOtx1*^{2}*/Otx2; Otx1*$^{-/-}$ 10.5 d.p.c. heads, neither an increase in OTX1 protein level nor its presence were detected in *hOtx1*^{2}*/Otx2; Otx1*$^{+/-}$ and *hOtx1*^{2}*/Otx2; Otx1*$^{-/-}$ embryos, respectively (Fig. 1H).

Therefore, in spite of the slight quantitative reduction and correct embryonic distribution of *hOtx1* mRNA, the hOTX1 protein was surprisingly undetectable. Moreover, also in *hOtx1*^{2}*/Otx2* ES cells, which normally synthesized the OTX2 protein, the *hOtx1* allele was correctly transcribed (data not shown) but the hOTX1 protein was not revealed (Fig. 1H).

hOtx1^{2}*/hOtx1*^{2} embryos developed a normal body axis but lacked anterior head structures

Since *hOtx1* was correctly transcribed but not translated, *hOtx1*^{2}*/hOtx1*^{2} embryos should show a phenotype similar or identical to that of *Otx2*$^{-/-}$ embryos (Fig. 2A). Surprisingly, at 8 d.p.c., as compared to wild type (Fig. 2B,C), *hOtx1*^{2}*/hOtx1*^{2} embryos displayed a quite normal morphology and only a slight reduction of neuroectodermal headfolds (Fig. 2F,G); at 8.5 d.p.c. wild-type (Fig. 2D,E) and mutant (Fig. 2H,I) embryos retained a similar body morphology but the rostral neuroectoderm of mutant embryos was reduced, abnormally folded and lacked prosencephalic features. At 10.5 d.p.c., the mutant phenotype (Fig. 2L,M) was evident and characterized by the absence of head structures rostral to the presumptive rhombomere 1 (see also below) while the body axis showed no obvious difference from the wild type (Fig. 2J,K). Moreover, in all the *hOtx1*^{2}*/hOtx1*^{2} embryos, heavy impairment of the maxillary process and mandibular arch were observed and, in ~50% of them, these structures were extremely reduced (Fig. 2M). About 50% of the expected *hOtx1*^{2}*/hOtx1*^{2} embryos reached the end of gestation showing a dramatic headless phenotype (Fig. 2O) even though ~15% of them showed residual, heavily abnormal craniofacial structures (data not shown). The variability in phenotype might likely correspond to incomplete penetrance of abnormality affecting neural crest cells and neuroectodermal territory from which they originate (see also the last paragraph of the Results section).

hOtx1 translation was restricted to the VE

The morphology of *hOtx1*^{2}*/hOtx1*^{2} embryos suggested that *hOtx1* mRNA should be translated at stages earlier than 8 d.p.c. when the endogenous *Otx1* gene is not transcribed. Hence, a detailed immunohistochemical analysis was performed on sections from wild type, *hOtx1*^{2}*/Otx2* and *hOtx1*^{2}*/hOtx1*^{2} gastrulating embryos. Genotypes of *hOtx1*^{2}*/Otx2* and *hOtx1*^{2}*/hOtx1*^{2} embryos were assessed by hybridizing adjacent sections with *hOtx1* (probe D in Fig. 1A) and *Otx2* (probe B

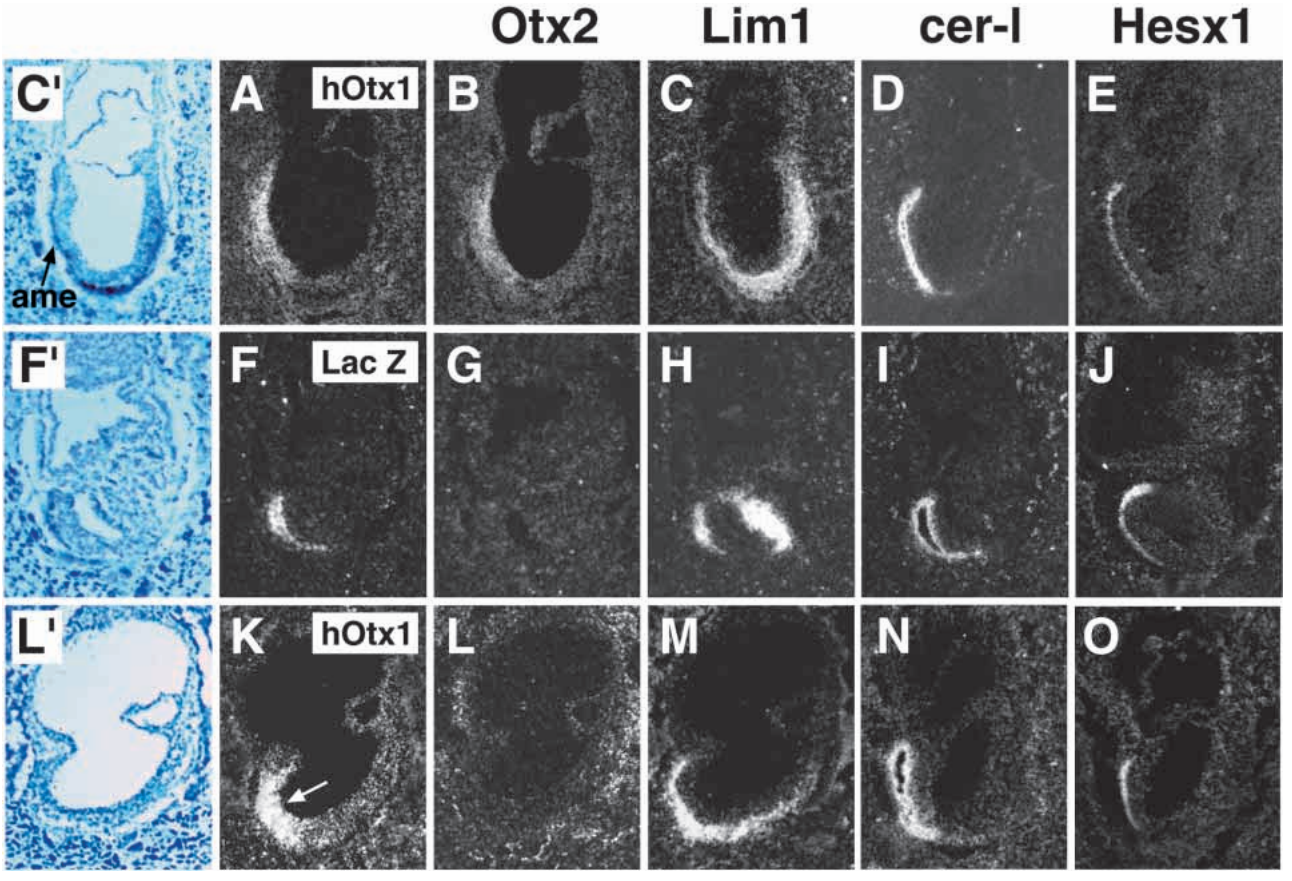

Fig. 5. *hOtx1*^{2}*/hOtx1*^{2} embryos correctly demarcate rostral ectoderm and recover axial mesendoderm. (A-O) Sagittal sections of 7. 5 d.p.c. *hOtx1*^{2}*/Otx2* (A-E), *Otx2*$^{-/-}$ (F-J) and *hOtx1*^{2}*/hOtx1*^{2} (K-O) embryos hybridized with *hOtx1* (A,K), *lacZ* (F), *Otx2* (B,G,L), *Lim1* (C,H,M), *cer-l* (D,I,N) and *Hesx1* (E,J,O) showing that *hOtx1* transcripts are correctly anteriorized (arrow in K), *Lim1* identifies axial mesoderm (M), *cer-l* the axial mesendoderm (N) and *Hesx1* the endoderm (O). (A-C, D,E, F-I, J, K-M, N,O) Single or group of sections belonging to different embryos. Bright fields of the same sections are labelled with a prime (′). Abbreviations as in previous figures.

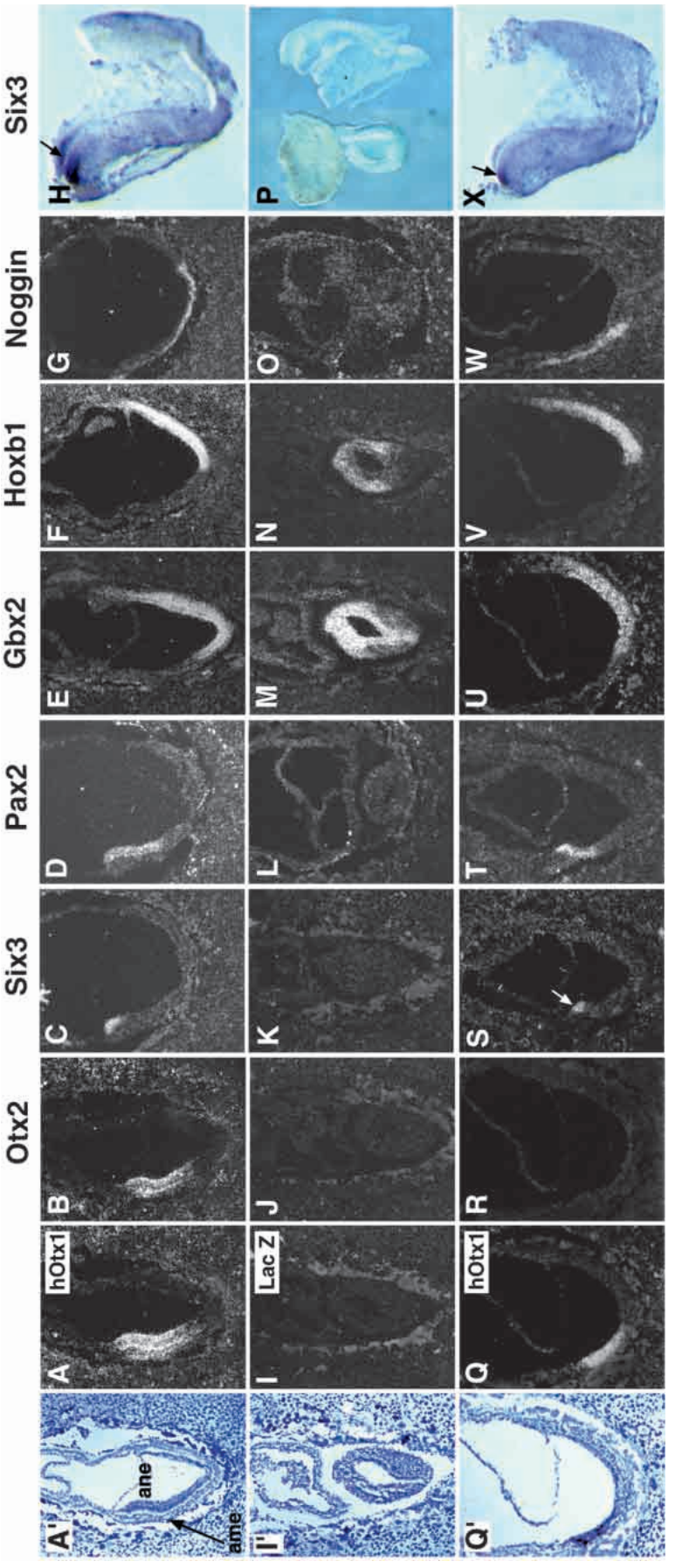

Fig. 6. *hOtx1^{2}/hOtx1^{2}* embryos recover initial patterning of the anterior neuroectoderm. (A-X) Sagittal sections of 7. 75 d.p.c. *hOtx1^{2}/Otx2* (A-G), *Otx2$^{-/-}$* (I-O) and *hOtx1^{2}/hOtx1^{2}* (Q-W) embryos hybridized with *hOtx1* (A,Q), *lacZ* (I), *Otx2* (B,J,R), *Six3* (C,K,S), *Pax2* (D,L,T), *Gbx2* (E,M,U), *Hoxb1* (F,N,V) and *Noggin* (G,O,W); at 8 d.p.c. as compared to *hOtx1^{2}/Otx2* (arrow in H), *Six3* still identifies rostral forebrain territory in *hOtx1^{2}/hOtx1^{2}* embryos (arrow in X) while no signal is detected in *Otx2$^{-/-}$* embryos at 8 (left) and 8. 5 (right) d. p. c., respectively (P). (A,B,E, C,D, F, G, I-K,M,N, L,O, Q,R,U,V, S,T, W) Single or group of sections belonging to different embryos. Bright fields of the same sections are labelled with a (′). Abbreviations as in previous figures.

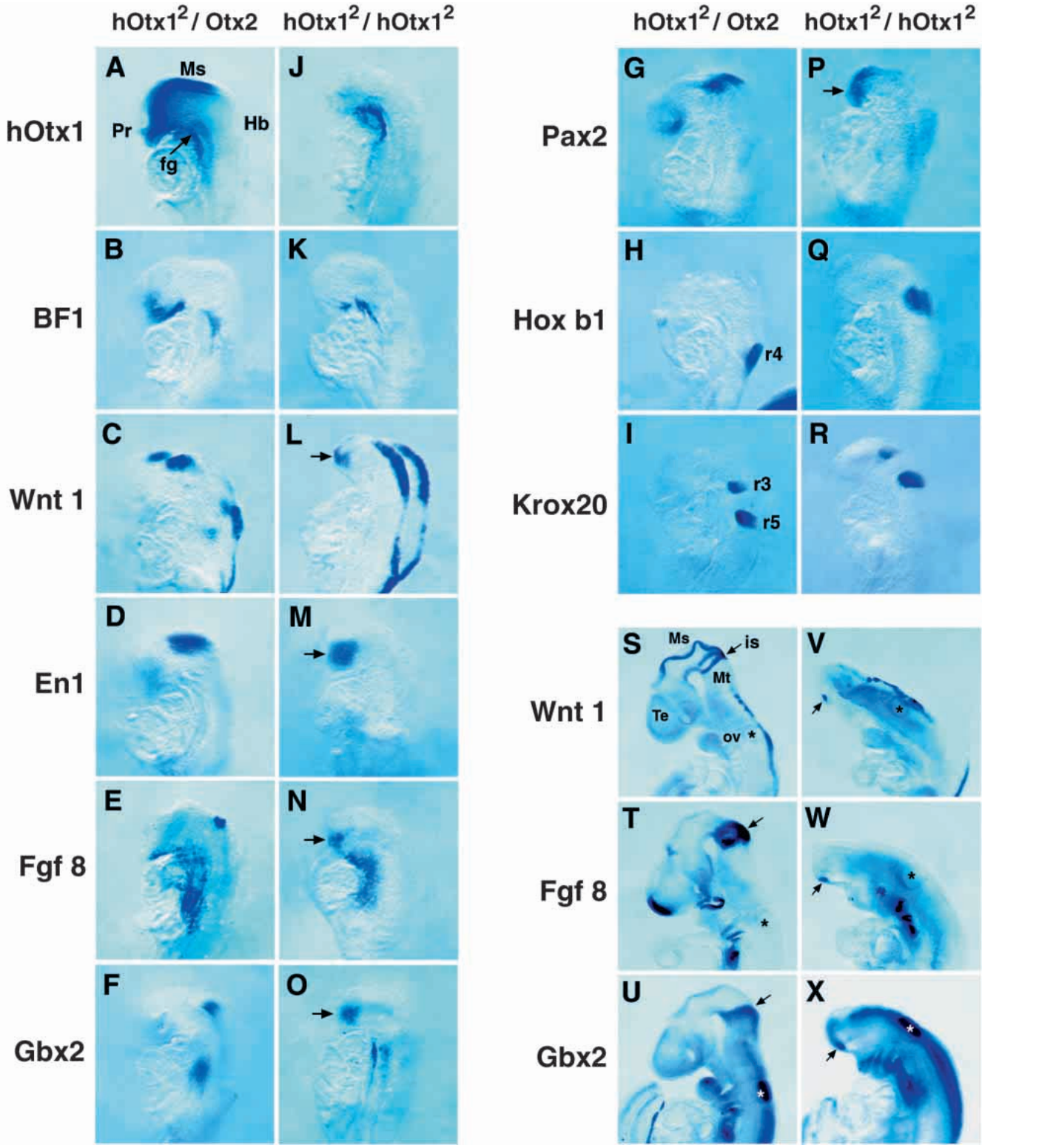

Fig. 7. *hOtx1^2/hOtx1^2* embryos lack forebrain-midbrain regional identities. (A-R) Whole-mount in situ hybridizations of 8. 5 d.p.c. *hOtx1^2/Otx2* (A-I) and *hOtx1^2/hOtx1^2* (J-R) embryos with *hOtx1* (A,J), *BF1* (B,K), *Wnt1* (C,L), *En1* (D,M), *Fgf8* (E,N), *Gbx2* (F,O), *Pax2* (G,P), *Hoxb1* (H,Q) and *Krox20* (I,R) showing that *hOtx1* and *BF1* transcripts disappear in the rostral neuroectoderm (J,K); *Wnt1, En1, Fgf8, Gbx2* and *Pax2* are transcribed at the rostral tip of the mutant embryos (arrows in L-P); *Hoxb1* and *Krox20* expression in rhombomeres 4 and 3, 5, respectively, are closer to the rostral limit of the mutant embryos (Q,R). (S-X) Whole-mount in situ hybridizations in 10. 5 d.p.c. *hOtx1^2/Otx2* (S-U) and *hOtx1^2/hOtx1^2* (V-X) embryos with *Wnt1* (S,V), *Fgf8* (T,W) and *Gbx2* (U,X) showing that a patch of cells located at the rostralmost tip of the mutant embryos expresses all of them (arrows in V-X). Abbreviations as in the previous figures plus: fg, foregut; r3, r4, r5 rhombomere 3, 4, 5; Mt, metencephalon. The asterisks label the otic vescicle (S-X) and the arrows in (S-U) point to the isthmus.

in Fig. 1A) allele-specific probes, respectively (see also Materials and Methods). In particular, the *Otx2* probe B contained a cDNA fragment that was deleted in the *Otx2* targeted locus (Fig. 1A) and identified only transcripts from the wild-type allele. Adjacent sections were assayed for immunodetection of OTX2 or hOTX1 proteins with an anti-OTX2 polyclonal antibody (αOTX2) or with an anti-OTX1 polyclonal antibody (αOTX1) exhaustively preabsorbed to pure recombinant OTX2 protein (αOTX1p). αOTX2 specificity was assessed on 7.5 d.p.c. $Otx2^{-/-}$ embryos (Fig. 3A). In wild-type embryos, *Otx2* mRNA and protein fully colocalized either in the VE and epiblast at 6.5 d.p.c. (Fig. 3B,C) or in the anterior neuroectoderm and axial mesendoderm at 7.75 d.p.c. (Fig. 3D-F). In $hOtx1^2/hOtx1^2$ embryos, at 6.5 d.p.c., *hOtx1* transcripts were detected either in the VE or in the epiblast cells (Fig. 3G) and, at 7.75 d.p.c., they were anteriorized in a region including presumptive rostral neuroectoderm and underlying presumptive axial mesendoderm (Fig. 3J). *Otx2* allele-specific probe did not reveal any signal (Fig. 3H,K).

Surprisingly, in contrast with the RNA distribution, hOTX1 protein revealed by the αOTX2 was restricted at 6.5 d.p.c. to the VE (Fig. 3I) and, at 7.75 d.p.c., only to a few cells in the most anteroproximal region of the embryo, which possibly corresponded to residual VE cells leaving the embryonic region (Fig. 3L,M). Western blots performed on $hOtx1^2/Otx2$ ES cells and head extracts from 10.5 d.p.c. embryos (Fig. 1M) already showed that the absence of the hOTX1 protein was independent of the presence of the OTX2 protein and should be mediated by an *hOtx1 cis*-acting mechanism. To confirm and extend this finding, the hOTX1 protein distribution was analyzed in 6.5 d.p.c. $hOtx1^2/Otx2$ embryos.

To perform this experiment, the αOTX1p specificity was assessed either by western blot assay on extracts from HeLa cells transfected with CMV-*hOtx1*- or *hOtx2*-expressing vectors or by immunohistochemical detection of OTX2 protein in wild-type embryos. Before being preabsorbed, the αOTX1 recognized both OTX1 and OTX2 proteins (Fig. 3N); after preabsorption, the αOTX1p clearly discriminated between OTX1 and OTX2, even though a faint OTX2 signal was still detectable either in western assay (Fig. 3N) or in wild-type 6.5 d.p.c. embryos (Fig. 3O), while no background was revealed in $Otx2^{-/-}$ embryos (Fig. 3P). The αOTX1p staining colocalized with the αOTX2, recognizing both OTX1 and OTX2 proteins, in $hOtx1^2/hOtx1^2$ embryos (data not shown).

At 6.5 d.p.c., in $hOtx1^2/Otx2$ embryos, *Otx2* and *hOtx1* mRNAs showed the same distribution in both VE and epiblast (Fig. 3Q,R). In contrast, while the αOTX2 detected OTX proteins in both VE and epiblast (Fig. 3S), the αOTX1p prevalently stained the VE (Fig. 3T). It is noteworthy that the faint signal detected in the epiblast by the αOTX1p (Fig. 3T) was likely due to a residual cross-reaction of the OTX2 protein.

Therefore, altogether these findings suggest that a differential post-transcriptional control, unmasked by the *hOtx1* chimaeric transcript, might exist between VE and epiblast cells, and indicate that the *Otx2* transcript escapes this post-transcriptional control in normal development. Moreover, the lack of hOTX1 protein in the epiblast and its derivatives is likely mediated by an OTX2-independent *cis*-acting control of the *hOtx1* mRNA.

$hOtx1^2/hOtx1^2$ embryos rescued *Otx2* requirements in VE

Previous data indicate an early requirement of *Otx2* in the VE (Acampora et al., 1995; Rhinn et al., 1998). Therefore, since the hOTX1 protein was restricted only to the VE, it enabled us to compare hOTX1 to OTX2 functional properties in the VE. To assess the genotype and to compare the expression pattern of different *Otx2* alleles (*hOtx1*, *lacZ*) to that of the wild-type *Otx2* gene, all the embryos deriving from $hOtx1^2/Otx2$ intercrosses were hybridized with *hOtx1* (probe D) and *Otx2* (probe B) allele-specific probes and those deriving from $Otx2^{+/-}$ intercrosses with *lacZ* and *Otx2* (probe B) probes.

Hence, the expression patterns of *hOtx1*, *Otx2*, *Lim1*, *Brachyury (T)*, *cerberus-like (cer-l)*, *Hesx1/Rpx (Hesx1)* and *goosecoid (gsc)* genes (Tam and Behringer, 1998; Belo et al., 1997 and references therein) were compared among the three genotypes corresponding to $hOtx1^2/Otx2$ (Fig. 4A-G), $Otx2^{-/-}$ (Fig. 4H-N) and $hOtx1^2/hOtx1^2$ (Fig. 4O-U).

At 6.5 d.p.c., in $hOtx1^2/Otx2$ embryos, *hOtx1* and *Otx2* transcripts colocalized throughout the epiblast and VE (Fig. 4A,B); *Lim1*, *cer-l*, *Hesx1* and *gsc* were expressed in the AVE (arrows in Fig. 4C,E,F,G), *gsc* and *Lim1* were also expressed in the early organizer cells (Fig. 4C,G) and *T* in the forming primitive streak (Fig. 4D).

In $Otx2^{-/-}$ embryos two major abnormalities were detected at this stage: (i) the *lacZ* reporting gene was expressed only in the VE (Acampora et al., 1995) (Fig. 4H), and (ii) the *gsc* transcripts were undetectable in most of the $Otx2^{-/-}$ embryos either in the VE or in the presumptive early organizer cells (Izpisuà-Belmonte et al., 1993; Fig. 4N) while, in the residual $Otx2^{-/-}$ embryos, a faint expression was detected in their proximal region (data not shown) (Acampora et al., 1995; Ang et al., 1996). Moreover, the expression of *Lim1*, *cer-l* and *Hesx1* appeared abnormally localized at the distal region of the embryo (Fig. 4J,L,M). The *T* gene was confined to the proximal region of the embryo (Fig. 4K). Interestingly, $hOtx1^2/hOtx1^2$ embryos rescued all the molecular and morphological abnormalities detected in the $Otx2^{-/-}$ embryos. Indeed, *hOtx1* transcripts were correctly detected either in the VE or throughout the epiblast (Fig. 4Q); *gsc* expression was rescued either in the early organizer cells or in the VE (Fig. 4U), and the VE-restricted expression of *Lim1*, *cer-l* and *Hesx1* was correctly anteriorized (arrows in Fig. 4Q,S,T).

At late streak stage (7.5 d.p.c.), in $hOtx1^2/Otx2$ embryos, *hOtx1* and *Otx2* transcripts were detected in the anterior third of the embryos (Fig. 5A,B), *Lim1* was expressed along the prechordal mesoderm (Fig. 5C), *cer-l* along the axial mesendoderm (Fig. 5D) and *Hesx1* was restricted to the endodermal cells (VE and definitive endoderm) (Fig. 5E).

In $Otx2^{-/-}$ embryos, rostral ectoderm and axial mesendoderm were severely impaired (Acampora et al., 1995; Matsuo et al., 1995; Ang et al., 1996). In fact, *lacZ* and *Lim1* transcripts were not detected in the presumptive rostral ectoderm and axial mesoderm, respectively (Fig. 5F,H) and became anteriorly coexpressed with *cer-l* (Fig. 5I) and *Hesx1* (Fig. 5J) suggesting that *lacZ*, *Lim1*, *cer-l* and *Hesx1* expression patterns colocalized in presumptive VE cells that still abundantly populated the anterior half of $Otx2^{-/-}$ embryos. Moreover, *Lim1* was also expressed posteriorly in mesoderm cells along the abnormal primitive streak (Fig. 5H).

Conversely, in *hOtx1²/hOtx1²* embryos *hOtx1* transcripts were properly restricted at the anterior third of the embryos in all three germ layers (Fig. 5K); *Lim1, cer-l* and *Hesx1* appeared correctly expressed in the axial mesoderm (Fig. 5M), axial mesendoderm (Fig. 5N) and endoderm cells (Fig. 5O), respectively.

These data indicate that OTX1 protein is sufficient to rescue *Otx2* requirements in the VE for proper gastrulation, demarcation of rostral ectoderm, as well as for its transcriptional maintenance in the epiblast cells. Moreover, from this data, it can be argued that OTX2 protein is apparently not required within the epiblast or its further derivatives for anterior demarcation of the rostral ectoderm.

hOtx1²/hOtx1² embryos showed anterior patterning of the early neural plate

At the headfold stage in *hOtx1²/Otx2* embryos, the anterior patterning of the neural plate was revealed by the forebrain-mid-hindbrain-restricted expression of several genes. In fact, *hOtx1* and *Otx2* expression patterns defined a broader area (Fig. 6A,B) including the forebrain-specific expression of *Six3* (Oliver et al., 1995) (Fig. 6C) and largely overlapping with that of *Pax2* (Rowitch and McMahon, 1995; Joyner, 1996) (Fig. 6D); more posteriorly, the border of the *Otx* transcripts (*hOtx1* and *Otx2*) was adjacent to the anterior one of *Gbx2* (Fig. 6E), which subsequently identifies the metencephalic component of the isthmus (Wassarman et al., 1997). Slightly more posteriorly, the anterior border of *Hoxb1* coincided with the presumptive rostral border of the rhombomere 4 (Fig. 6F) (Wassarman et al., 1997). All these regional identities were lost in 7.75 d.p.c. *Otx2*$^{-/-}$ embryos where *lacZ, Six3* and *Pax2* transcripts were undetectable (Fig. 6I,K,L) while *Gbx2* (Fig. 6M) was expressed throughout all the presumptive neuroectoderm and proximal mesoderm and *Hoxb1* even more proximally in both neuroectoderm and mesoderm (Fig. 6N). The presence of neuroectoderm tissue was deduced by the expression of the early panneural marker *Sox2* (data not shown). In *hOtx1²/hOtx1²* embryos, *hOtx1* was transcribed in the rostral neuroectoderm and in the underlying presumptive axial mesendoderm (Fig. 6Q). However, *Six3* (Fig. 6S) and *Pax2* (Fig. 6T) were correctly detected in the rostral neuroectoderm territory expressing *hOtx1*, and more posteriorly *Gbx2* (Fig. 6U) and *Hoxb1* (Fig. 6V) showed a basically normal expression pattern retaining their relative territorial relationships with the *hOtx1* expression domain. Furthermore, in *hOtx1²/hOtx1²* embryos, the forebrain-specific expression of *Six3* was still detected at 8 d.p.c. (Fig. 6X), even though the expressing territory was smaller compared to that of *hOtx1²/Otx2* embryos (Fig. 6H). This reduction might be also due to a decreased proliferating activity within the rostral neuroectoderm that normally should express *Otx2*.

Finally, to assess the proper identity of axial mesoderm, the expression pattern of *Noggin* was analyzed (Smith and Harland, 1992; McMahon et al., 1998; Rhinn et al., 1998). *Noggin* transcripts were detected along the axial mesoderm in both *hOtx1²/Otx2* (Fig. 6G) and, importantly, *hOtx1²/hOtx1²* (Fig. 6W) embryos, while they were not revealed in *Otx2*$^{-/-}$ embryos (Fig. 6O). These findings indicate that severe impairments, such as lack of both rostral neuroectoderm and axial mesendoderm affecting *Otx2*$^{-/-}$ embryos, were rescued by the VE-restricted OTX1 protein.

Patterning of the anterior neural plate was not maintained in *hOtx1²/hOtx1²* embryos

The early neural plate undergoes additional morphogenetic changes which gradually refine the anteroposterior (A/P) patterning (reviewed in Rubenstein et al., 1998).

A/P regional identities of the *hOtx1²/hOtx1²* neural plate were assessed at 8.5 and 10.5 d.p.c. by analyzing the expression of a number of genes restricted to forebrain, midbrain and hindbrain territories. At 8.5 d.p.c., in *hOtx1²/Otx2* embryos *hOtx1* transcripts identified forebrain-midbrain territories (Fig. 7A), *BF1* (Fig. 7B) – the rostral forebrain, *Wnt1* – the midbrain (Fig. 7C), *En1* – the posterior midbrain and rostral hindbrain (Fig. 7D), *Fgf8, Gbx2* and *Pax2* – a more restricted area including the isthmic primordium at the mes-met boundary (Fig. 7E-G) (Rowitch and McMahon, 1995; Crossley et al., 1996; Joyner, 1996; Wassarmann et al., 1997; Rubenstein et al., 1998) and, finally, *Hoxb1* and *Krox20* – rhombomeres 4 and 3, 5, respectively (Fig. 7H,I) (Lumsden and Krumlauf, 1996). Interestingly, in *hOtx1²/hOtx1²* embryos, *hOtx1* and *BF1* (Fig. 7J,K) transcripts were not detected in the rostral neuroectoderm while they were still present in the foregut and anteriormost ectoderm, respectively (Fig. 7J,K); *Wnt1, En1, Fgf8, Gbx2* and *Pax2* were expressed altogether at the rostral tip of the embryo (Fig. 7L-P); *Hoxb1* and *Krox20* stripes appeared closer to the rostral end of the embryo (Fig. 7Q,R).

It is noteworthy that ~50% of the mutant embryos hybridized with the *Wnt1* probe did not reveal any signal at the rostral tip of the embryos (data not shown). Moreover, since the *Otx* transcripts were never detected in *hOtx1²/hOtx1²* embryos, the *Wnt1* expression might be likely due to an *Fgf8*-mediated local induction rather than be associated with a residual midbrain territory. Finally, at 10.5 d.p.c. when the headless phenotype was evident, *Wnt1, Fgf8* and *Gbx2* were coexpressed at the very rostral tip of most of the *hOtx1²/hOtx1²* embryos (60%) in a small patch of cells (arrows in Fig. 8V-X). In the residual embryos, this rostral expression was not detected (data not shown). From these findings, it can be argued that OTX2 gene product is required from the headfold stage onwards to maintain the anterior patterning previously established. In this respect, the phenotype observed at 8.5 d.p.c. appears to be the consequence of an A/P repatterning process involving all the anterior neural plate (forebrain-midbrain) which, in the absence of any OTX gene product, adopts a more posterior fate (hindbrain). It should be noted that the repatterned neuroectoderm might likely be abnormal and that these abnormalities may be reflected in heavy impairments of branchial arches.

DISCUSSION

VE-restricted OTX1 protein recovers *Otx2* requirements in the VE

The aim of this work was to compare functional properties of *Otx1* to those of *Otx2*. Here we reported that VE-restricted OTX1 protein is sufficient to rescue VE-restricted requirements of *Otx2* for proper gastrulation and early specification of the rostral neural plate, indicating that *Otx1* and *Otx2* functional properties largely overlap in the VE and,

therefore, that their transcriptional control rather than the limited amino acid divergence is responsible for the highly divergent phenotypes observed in mice lacking *Otx1* or *Otx2* (Acampora et al., 1995, 1996; Matsuo et al., 1995; Ang et al., 1994). The analysis of *Otx2* null embryos revealed that, at late streak stage, the rostral neuroectoderm was not identified and the primitive streak as well as node-derived cells of the axial mesendoderm were severely impaired. However, in embryos replacing *Otx2* with a *lacZ* reporting gene, the first abnormality was already detected at the early streak stage (Acampora et al., 1995). At this stage, *lacZ* staining and transcription were abolished in the epiblast while they remained high in the VE of $Otx2^{-/-}$ embryos. Furthermore, *goosecoid (gsc)* expression in early node-precursor cells having inducing properties (Izpisùa-Belmonte et al., 1993), was undetectable or confined to the proximal region of the embryo.

Thus, since *Otx2* is already transcribed from the earliest stages – in mouse at least at the morula stage (data not shown) – these data indicate that maintenance of *Otx2* transcription in the epiblast cells requires at least one normal allele expressed in the VE, while transcription of the *Otx2* locus in the VE is independent of the presence of a normal allele. Therefore, abnormal primitive streak organization and headless phenotype might be determined very early at the pre-early streak stages by an impairment of VE-restricted properties of *Otx2*. In this context, it is noteworthy that the chick hypoblast is required for the correct organization of the primitive streak (Stern, 1992) and that, therefore, chick hypoblast and murine VE might share similar roles.

Furthermore, a role for *Otx2* in the AVE has been recently provided by generating murine chimaeric embryos containing $Otx2^{-/-}$ epiblast cells and wild-type VE or vice versa (Rhinn et al., 1998). In these experiments, the wild-type VE was sufficient to rescue an early neural plate, thus suggesting that an *Otx2*-mediated role of the VE is required in early neural plate specification. Additional remarkable evidence indicates that, in mouse, the AVE and, in *Xenopus*, the leading edge of the involuting endoderm play a crucial role in head organizer activity. (i) In mouse, transplantation of node-derived axial mesoderm induces a secondary axis lacking anteriormost neural tissues (Beddington, 1994). (ii) Removal of a patch of cells expressing the *Hesx1* gene prevents the subsequent expression of the gene in the rostral headfolds which result reduced and abnormally patterned (Thomas and Beddington, 1996; Dattani et al., 1998). (iii) Chimaeric embryos composed of wild-type epiblast and $nodal^{-/-}$ visceral endoderm result heavily impaired in rostral CNS development (Varlet et al., 1997). (iv) In *Xenopus*, the secreted molecule coded by the *cerberus* gene is restricted to the leading edge of the involuting endoderm and microinjection of its mRNA into embryos induces the formation of ectopic head-like structures (Bouwmeester et al., 1996). (v) Most of the genes expressed in the node or in the axial mesendoderm cells are also expressed in the AVE, thus reinforcing the idea that, in mouse, the organizer might be split into at least two embryonic regions operating at different stages to specify head and trunk organizer signals (Thomas and Beddington, 1996; Belo et al., 1997; Ruiz i Altaba, 1998).

We reported that, unexpectedly, in spite of the correct distribution of *hOtx1* mRNA, the protein was exclusively detected in the VE of homozygous mutant embryos (see also below). This restricted and transient presence of the hOTX1 protein is sufficient to recover early abnormalities affecting *Otx2* null embryos.

Moreover, the VE-restricted hOTX1 protein is also sufficient to mediate maintenance of *hOtx1* transcription in the epiblast cells.

Interestingly, in $hOtx1^2/hOtx1^2$ embryos at the headfold stage *hOtx1* expression domain included rostral neuroectoderm fated to give forebrain-midbrain and underlying axial mesendoderm. At this stage, *Lim1, Noggin, cer-l* and *Hesx1* are properly expressed in axial mesendoderm components and *Six3, Pax2, Gbx2* and *Hoxb1* correctly define the anterior patterning of the neural plate leading us to argue that, in wild-type embryos, OTX2 protein is required in the VE but not in epiblast or node-derived axial mesendoderm for the initial patterning and demarcation of rostral neuroectoderm. In this respect, it is worth noting that *Otx2, Lim1, gsc, Hesx1* and the murine *cer-l* genes are all coexpressed in the AVE, thus suggesting that they may overlap in the earliest genetic pathway involved in organizing the head (Thomas and Beddington, 1996; Belo et al., 1997; Tam and Behringer, 1997).

Otx2 is required for maintenance of anterior patterning

At the headfold stage, the rostral neuroectoderm where *hOtx1* was transcribed displayed an anterior patterning but failed in its maintenance. At late gastrula/headfold stage *Otx2* is normally transcribed and translated in both axial mesendoderm and rostral neuroectoderm suggesting that it is required in one or both tissues.

Evidence so far provided does not exclude either a role in the axial mesendoderm (Ang et al., 1994; Simeone et al., 1995; Avantaggiato et al., 1996) or within the rostral neuroectoderm (Acampora et al., 1997; Rhinn et al., 1998). Here, we provide strong evidence that *Otx2* is required from the headfold stage onwards (up to the 5- to 6-somite stage) to maintain anterior patterning of the neural plate that otherwise acquires a more posterior fate. Nevertheless, it cannot be argued from our data in which tissue (axial mesendoderm and/or neuroectoderm) *Otx2* is required. Recent evidence in chick embryos indicates that the prechordal region does not have neural-inducing properties while it is able to confer anterior character to prospective posterior neuroepithelium (hindbrain) by activating the expression of *Otx2* and *tailless* genes (Foley et al., 1997).

Finally, it is noteworthy that *Lim1* is correctly expressed in the prechordal mesoderm of $hOtx1^2/hOtx1^2$ embryos and that $Lim1^{-/-}$ (Shawlot and Behringer, 1995) and $hOtx1^2/hOtx1^2$ embryos show impressive phenotypic similarities. On this basis, it can be speculated that *Lim1* might mediate the ability of prechordal mesoderm in instructing maintenance of anterior character and *Otx2* might confer to neuroectoderm the competence in responding to the maintenance signal from mesendoderm. In summary, our mouse model allows us to uncouple two distinct phases: early induction of anterior neural patterning that appears to be under the control of VE and its subsequent maintenance that is likely mediated by epiblast-derived cells (the axial mesendoderm and neuroectoderm).

Differential post-transcriptional control of *Otx1* between VE and epiblast

Our data showed that the hOTX1 protein was restricted to the

VE even though its mRNA was detected in both VE and epiblast.

In wild-type embryos, *Otx2* mRNA and protein colocalized during gastrulation indicating that *Otx2* escapes this post-transcriptional control. Moreover, western blot analysis and in situ detection of OTX1 and OTX2 proteins suggest that the *hOtx1* chimaeric transcript is post-transcriptionally regulated by an *Otx2*-independent *cis*-acting control.

In $Otx2^{+/-}$ embryos, the same *Otx2* region that is replaced in the present work by the *hOtx1* cDNA was substituted with the *lacZ* gene fused to the SV40 poly(A) site (Acampora et al., 1995). In these embryos ($Otx2^{+/-}$), the *lacZ* mRNA was correctly detected in VE and epiblast while the staining was heavily reduced in the epiblast at early-mid streak stage (Acampora et al., 1995). These previous findings and those reported here suggest that the *Otx2* replaced region, possibly the 3′ UTR, might contain regulatory element(s) required for the *Otx2* translation in the epiblast cells. However, such molecular element(s) is actually unknown and in vivo experiments performed by generating mouse models specifically addressing this issue will certainly contribute toward unmasking eventual post-transcriptional control element(s) that at the moment can be only hypothesized. Alternatively, since the *Otx2* locus is heavily engineered in our mouse model and the *hOtx1* cDNA does not contain introns or either the 3′ UTR and part of the 5′ UTR of the *Otx2* locus, it could be possible that the loss of hOTX1 protein in the epiblast might be mediated by abnormal molecular event(s) affecting RNA stability, processing, transport or translation of the chimaeric *hOtx1* transcript. Nevertheless, since in the VE the *hOtx1* mRNA is correctly translated, the absence of hOTX1 protein should be considered a peculiar event occurring in epiblast cells and their derivatives. However, new mouse models carrying the *Otx2* cDNA with and/or without its 5′ and 3′ UTRs into a disrupted *Otx2* locus will be necessary to assess the real contribution of introns and untranslated regions of *Otx2* in generating the phenotype of $hOtx1^2/hOtx1^2$ embryos.

We thank S.-L. Ang, G. Grimaldi, M. Gulisano, S. Martinez and H. Reichert for helpful discussions. We are also indebted to R. Beddington for the *cer-l* and *Hesx1* probes. We are grateful to A. Secondulfo for typing the manuscript. This work was supported by grants from the Italian Telethon Program, The Italian Association for Cancer Research (AIRC), the 'CNR Target Project on Biotechnology' and the EC BIOTECH Programme.

REFERENCES

Acampora, D., Mazan, S., Lallemand, Y., Avantaggiato, V., Maury, M., Simeone, A. and Brûlet, P. (1995). Forebrain and midbrain regions are deleted $Otx2^{-/-}$ mutants due to a defective anterior neuroectoderm specification during gastrulation. *Development* **121**, 3279-3290.

Acampora, D., Mazan, S., Avantaggiato, V., Barone, P., Tuorto, F., Lallemand, Y., Brûlet, P. and Simeone, A. (1996). Epilepsy and brain abnormalities in mice lacking *Otx1* gene. *Nature Genet.* **14**, 218-222.

Acampora, D., Avantaggiato, V., Tuorto, F. and Simeone, A. (1997). Genetic control of brain morphogenesis through *Otx* gene dosage requirement. *Development* **124,** 3639-3650.

Acampora, D., Mazan, S., Tuorto, F., Avantaggiato, V., Tremblay, J. J., Lazzaro, D., di Carlo, A., Mariano, A., Macchia, P. E., Corte, G., Macchia, V., J. Drouin, J., Brûlet, P. and Simeone, A. (1998). Transient dwarfism and hypogonadism in mice lacking *Otx1* reveal prepubescent stage-specific control of pituitary levels of GH, FSH and LH. *Development* **125**, 1061-1072.

Ang, S.-L., Conlon, R. A., Jin, O. and Rossant, J. (1994). Positive and negative signals from mesoderm regulate the expression of mouse *Otx2* in ectoderm explants. *Development* **120**, 2979-2989.

Ang, S.-L., Jin, O., Rhinn, M., Daigle, N., Stevenson, L. and Rossant, J. (1996). Targeted mouse *Otx2* mutation leads to severe defects in gastrulation and formation of axial mesoderm and to deletion of rostral brain. *Development* **122**, 243-252.

Avantaggiato,V., Acampora, D., Tuorto, F. and Simeone, A. (1996). Retinoic acid induces stage-specific repatterning of the rostral central nervous system. *Dev. Biol.* **175**, 347-357.

Barnes, J. D., Crosby, J. L., Jones, C. M., Wright, C. V. and Hogan, B. L. (1994). Embryos expression of Lim-1, the mouse homolog of Xenopus Xlim-1, suggests a role in lateral mesoderm differentiation and neurogenesis. *Dev. Biol.* **161**, 167-178.

Beddington, R. S. P. (1994). Induction of a second neural axis by the mouse node. *Development* **120**, 613-620.

Belo, J. A., Bouwmeester, T., Leyns, L., Kertesz, N., Gallo, M., Gollettie, M. and De Robertis, E. M. (1997). *Cerberus-like* is a secreted factor with neuralizing activity expressed in the anterior primitive endoderm of the mouse gastrula. *Mech. Dev.* **68**, 45-57.

Bouwmeester, T., Kim, S. H., Sasai, Y., Lu, B. and De Robertis, E. M. (1996). Cerberus is a head-inducing secreted factor expressed in the anterior endoderm of Spemann's organizer. *Nature* **382**, 595-601.

Chapman, G., Remiszeski, J. L., Webb, G. C., Schultz, T. C., Bottema, C. D. and Rathjen, P. D. (1997). The mouse homeobox gene, *Gbx2*: genomic organization and expression in pluripotent cells in vitro and in vivo. *Genomics* **46**, 223-233.

Chen, S., Wang, Q.-L., Nie, Z., Sun, H., Lennon, G., Copeland, N. G., Gilbert, D. J., Jenkins, N. A. and Zack, D. J. (1997). Crx, a novel Otx-like paired-homeodomain protein, binds to and transactivates photoreceptor cell-specific genes. *Neuron* **19**, 1017-1030.

Crossley, P. H., Martinez S. and Martin, G. R. (1996). Midbrain development induced by FGF8 in the chick embryo. *Nature* **380**, 66-68.

Dattani, M. T., Martinez-Barbera, J.-P., Thomas, P. Q., Brickman, J. M., Gupta, R., Mårtensson, I.-L., Toresson, H., Fox, M., Wales, J. K. H., Hindmarsh, P. C., Krauss, S., Beddington R. S. P. and Robinson, I. C. A. F. (1998). Mutations in the homeobox gene *HESX1/Hesx1* associated with septo-optic dysplasia in human and mouse. *Nat. Genet.* **19**, 125-133.

Doniach, T. (1993). Planar and vertical induction of anteroposterior pattern during the development of the amphibian central nervous system. *J. Neurobiol.* **24**, 1256-1276.

Finkelstein, R. and Boncinelli, E. (1994). From fly head to mammalian forebrain: the story of *otd* and *Otx*. *Trends Genet.* **10**, 310-315.

Foley, A. C., Storey, K. G. and Stern, C. D. (1997). The prechordal region lacks neural inducing ability, but can confer anterior character to more posterior neuroepithelium. *Development* **124**, 2983-2996.

Frantz, G. D., Weimann, J. M., Levin, M. E. and McConnell, S. K. (1994). *Otx1* and *Otx2* define layers and regions in developing cerebral cortex and cerebellum. *J. Neurosci.* **14**, 5725-5740.

Freud, C. L., Gregory-Evans, C. Y., Kurukawa, T., Papaioannou, M., Looser, J., Ploder, L., Bellingham, J., Ng, D., Herbrick, J.-A. S., Duncan, A., Scherer, S. W., Tsui, L.-C., Loutradis-Anagnostou, A., Jacobson, S. G., Cepko, C. L., Bhattacharya, S. S. and McInnes, R. R. (1997). Cone-rod dystrophy due to mutations in a novel photoreceptor-specific homeobox gene (*CRX*) essential for maintenance of the photoreceptor. *Cell* **91**, 543-553.

Gurdon, J. B. (1987). Embryonic induction – molecular prospects. *Development* **99,** 285-306.

Hogan, B., Beddington, R., Costantini, F. and Lacy, E. (1994). In *Manipulating the Mouse Embryo. A Laboratory Manual.* 2nd edn. Cold Spring Harbor Laboratory Press.

Houart, C., Westerfield, M. and Wilson, S. W. (1998). A small population of anterior cells patterns the forebrain during zebrafish gastrulation. *Nature* **391**, 788-792.

Joyner, A. L. (1996). *Engrailed, Wnt* and *Pax* genes regulate midbrain-hindbrain development. *Trends Genet.* **12**, 15-20.

Izpisùa-Belmonte, J. C., De Robertis, E. M., Storey, K. G. and Stern, C. D. (1993). The homeobox gene *goosecoid* and the origin of the organizer cells in the early chick blastoderm. *Cell* **74**, 645-659.

Lemaire, P. and Kodjabachian, L. (1996). The vertebrate organizer: structure and molecules. *Trends Genet.* **12**, 525-531.

Li, H., Tao, W. and Lai, E. (1996). Characterization of the structure and

function of the gene for transcription factor BF-1, an essential regulator of forebrain development. *Brain Res. Mol. Brain Res.* **37**, 96-104.

Logan, C., Hanks, M. C., Noble-Topham, S., Nallainathan, D., Provart, N. J. and Joyner, A. L. (1992). Cloning and sequence comparison of the mouse, human, and chicken engrailed genes reveal potential functional domains and regulatory regions. *Dev. Genet.* **13**, 345-358.

Lumsden A. and Krumlauf, R. (1996). Patterning the vertebrate neuraxis. *Science* **274**, 1109-1115.

Mallamaci, A., Di Blas, E., Briata, P., Boncinelli, E. and Corte, G. (1996). OTX2 homeoprotein in the developing central nervous system and migratory cells of the olfactory area. *Mech. Dev.* **58**, 165-178.

Matsuo, I., Kuratani, S., Kimura, C., Takeda, N. and Aizawa, S. (1995). Mouse *Otx2* functions in the formation and patterning of rostral head. *Genes Dev.* **9**, 2646-2658.

McMahon, J. A., Takada, S., Zimmerman, L. B., Fan, C.-M., Harland, R. M. and McMahon, A. P. (1998). Noggin-mediated antagonism of BMP signaling is required for growth and patterning of the neural tube and somite. *Genes Dev.* **12**, 1438-1452.

Millet, S., Bloch-Gallego, E., Simeone, A. and Alvarado-Mallart, R.-M. (1996). Is the caudal limit of *Otx2* gene expression a marker of the midbrain/hindbrain boundary? A study using a chick-*Otx2* riboprobe and chick/quail homotopic grafts. *Development* **122**, 3785-3797.

Oliver, G., Mailhos, A., Wehr, R., Copeland, N. G., Jenkins, N. A. and Gruss, P. (1995). Six3, a murine homologue of the sine oculis gene, demarcates the most anterior border of the developing neural plate and is expressed during eye development. *Development* **121**, 4045-4055.

Rhinn, M., Dierich, A., Shawlot, W., Behringer, R. R., Le Meur, M. and Ang, S.-L. (1998). Sequential roles for Otx2 in visceral endoderm and neuroectoderm for forebrain and midbrain induction and specification. *Development* **125**, 845-856.

Rowitch, D. H. and McMahon, A. P. (1995). *Pax-2* expression in the murine neural plate precedes and encompasses the expression domains of *Wnt1* and *En1*. *Mech. Dev.* **52,** 3-8.

Rubenstein, J. L. R., Shimamura, K., Martinez, S. and Puelles, L. (1998). Regionalization of the prosencephalic neural plate. *Annu. Rev. Neurosci.* **21**, 445-477.

Ruiz i Altaba, A. (1993). Induction and axial patterning of the neural plate: planar and vertical signals. *J. Neurobiol.* **24**, 1276-1304.

Ruiz i Altaba, A. (1994). Pattern formation in the vertebrate neural plate. *Trends Neurosci.* **17**, 233-243.

Ruiz i Altaba, A. (1998). Deconstructing the organizers. *Nature* **391**, 748-749.

Shawlot, W. and Behringer, R. R. (1995). Requirement for *Lim1* in head organizer function. *Nature* **374**, 425-430.

Simeone, A., Acampora, D., Gulisano, M., Stornaiuolo, A. and Boncinelli, E. (1992). Nested expression domains of four homeobox genes in developing rostral brain. *Nature* **358**, 687-690.

Simeone, A., Acampora, D., Mallamaci, A.,Stornaiuolo, A., D'Apice, M. R., Nigro, V. and Boncinelli, E. (1993). A vertebrate gene related to *orthodenticle* contains a homeodomain of the *bicoid* class and demarcates anterior neuroectoderm in the gastrulating mouse embryo. *EMBO J.* **12,** 2735-2747.

Simeone, A., Avantaggiato, V., Moroni, M. C., Mavilio, F., Arra, C., Cotelli, F., Nigro, V. and Acampora, D. (1995). Retinoic acid induces stage-specific antero-posterior transformation of rostral central nervous system. *Mech. Dev.* **51,** 83-98.

Smith, W. C. and Harland, R. M. (1992). Expression cloning of noggin, a new dorsalizing factor localized to the Spemann orgnaizer in Xenopus embryos. *Cell* **70**, 829-840.

Spemann, H. and Mangold, H. (1924). Über induktion von Embryonanlagen durch Implantation artfremder Organisatoren. *Wilhelm Roux Arch. EntwMech. Organ.* **100**, 599-638.

Stern, C. D. (1992). Mesoderm induction and development of the embryonic axis in amniotes. *Trends Genet.* **8**, 158-163.

Tam, P. P. L. and Behringer, R. R. (1997). Mouse gastrulation: the formation of a mammalian body plan. *Mech. Dev.* **68**, 3-25.

Thomas, P. and Beddington, R. (1996). Anterior primitive endoderm may be responsible for patterning the anterior neural plate in the mouse embryo. *Curr. Biol.* **6,** 1487-1496.

Varlet, I., Collignon, J. and Robertson, E. J. (1997). *nodal* expression in the primitive endoderm is required for specification of the anterior axis during mouse gastrulation. *Development* **124**, 1033-1044.

Waddington, C. H. (1932). Experiments on the development of chick and duck embryos, cultivated *in vitro*. *Phil. Trans. Roy. Soc. Lond. B* **221**, 179-230.

Wassarman, K. M., Lewandoski, M., Campbell, K., Joyner, A. L., Rubenstein, J. L. R., Martinez, S. and Martin, G. R. (1997). Specification of the anterior hindbrain and establishment of a normal mid/hindbrain organizer is dependent on *Gbx2* gene function. *Development* **124,** 2923-2934.

Wilkinson, D. G. (1992). Whole mount *in situ* hybridization of vertebrate embryos. In *In Situ Hybridization: A Practical Approach*, Oxford: IRL, Oxford University Press.